American Mineralogist, Volume 88, pages 782–788, 2003

Neutron and temperature-resolved synchrotron X-ray powder diffraction study of akaganéite

JEFFREY E. POST,[1,*] PETER J. HEANEY,[2] ROBERT B. VON DREELE,[3] AND JONATHAN C. HANSON[4]

[1]Department of Mineral Sciences, Smithsonian Institution, Washington, D.C. 20560-0119, U.S.A.
[2]Department of Geosciences, 309 Deike, Pennsylvania State University, University Park, Pennsylvania 16802, U.S.A.
[3]LANSCE-12, MS H805, Los Alamos National Laboratory, Los Alamos, New Mexico 87545, U.S.A.
[4]Chemistry Department, Brookhaven National Laboratory, Upton, New York 11793, U.S.A.

ABSTRACT

Rietveld refinements using neutron powder diffraction data were used to locate H atom positions and obtain a more precise crystal structure refinement for akaganéite [$Fe^{3+}_{7.6}Ni^{2+}_{0.4}O_{6.35}(OH)_{9.65}Cl_{1.25}\cdot nH_2O$]. Difference Fourier maps clearly showed H atoms positions near those O atoms at the midpoints of the tunnel edges. The O-H vectors point toward the Cl sites at the center of the tunnel, and weak hydrogen bonds likely form between the framework O atoms and Cl. The Cl position is near the center of a prism defined by the eight hydroxyl H atoms. The Cl atoms fill ~2/3 of the tunnel sites, suggesting an ordering scheme in a given tunnel with every third tunnel site vacant. Such an arrangement allows the Cl anions to increase their separation distance along a tunnel by displacing away from one another toward their respective adjacent vacancies. The Fe-O octahedra in akaganéite are distorted with Fe-(O, OH) distances ranging from 1.94 to 2.13 Å and show three longer and three shorter Fe-O distances; as expected the longer distances are associated with the OH^- anions.

Temperature-resolved synchrotron X-ray powder diffraction data and Rietveld refinements were used to investigate changes in the akaganéite structure and its transformation into hematite as it was heated from 26 to 800 °C. Rietveld refinements revealed surprising consistency in all unit-cell parameters between room temperature and ~225 °C, resulting in nearly zero thermal expansion of the akaganéite structure over a 200 °C interval. Above ~225 °C, the unit-cell volume gradually decreased, primarily in response to decreases in *c* and *b*, and an increase in the β angle. The *a* parameter remained nearly constant until ~225 °C and increased thereafter. Akaganéite started to transform to hematite in the temperature range 290 to 310 °C with no evidence for maghemite as an intermediate phase.

INTRODUCTION

Akaganéite is the naturally occurring form of β-FeOOH and has been recognized as a significant Fe-oxide component in soils and geothermal brine deposits (Holm et al. 1983) and as a corrosion product of some steels and iron meteorites (Buchwald and Clarke 1989). Both natural and synthetic akaganéite typically occurs as fine-grained masses, and no crystals have been found that are suitable for single-crystal diffraction studies. Post and Buchwald (1991) performed a Rietveld refinement using powder X-ray diffraction data from akaganéite [$Fe^{3+}_{7.6}Ni^{2+}_{0.4}O_{6.35}(OH)_{9.65}Cl_{1.25}\cdot nH_2O$] from the Campo del Cielo meteorite. They confirmed the hollandite-type structure, in which double chains of edge-linked Fe^{3+}-(O, OH) octahedra share corners to form a framework containing large tunnels with square cross sections that measure two octahedra per side (Fig. 1). The Cl atoms reside in the tunnels, and the negative charges introduced by the Cl atoms are offset by substitution of higher-valence cations into the octahedral sites, or by additional H atoms. Post and Buchwald (1991) also showed that the structure has monoclinic symmetry (*I*2/*m*), not tetragonal as was previously assumed (Keller 1970). The akaganéite structure is unusual among known hollandite-type phases in that the framework cations (Fe^{3+}) are predominantly trivalent rather than quadravalent, and the tunnels contain anions (Cl^-) rather than cations.

Because of limitations imposed by the use of powder X-ray diffraction data, Post and Buchwald (1991) were not able to locate H atom positions in the akaganéite structure; also, some of the Fe-(O,OH) distances were anomalously long compared with those in similar iron hydroxide phases. Consequently, in an attempt to locate H atom positions and obtain a more precise crystal structure refinement, we undertook a neutron powder diffraction study of akaganéite. In addition to its advantage for use in locating H atoms, the neutron data offered improved precision for light element positions, such as for O atoms. Our study challenged two of the general tenets of powder neutron diffraction experiments: (1) that large amounts of sample (on the order of grams) are required, and (2) that usable data cannot be collected from H-rich samples because of the high incoherent scattering contribution to the background by H atoms. The neutron data for this study were collected from an ~100

* E-mail: post.jeffrey@nmnh.si.edu

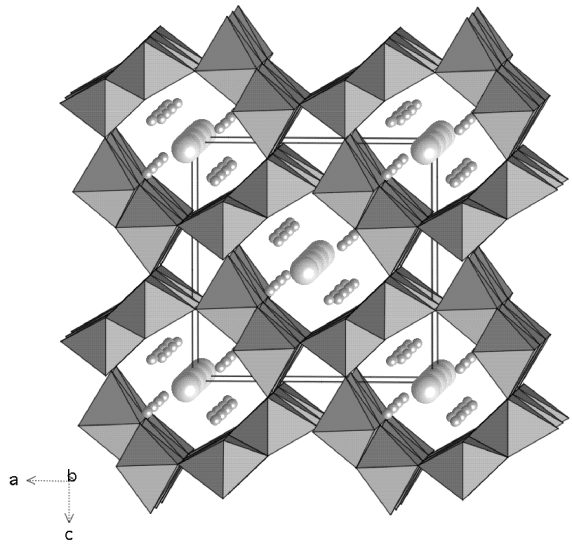

FIGURE 1. Polyhedral representation of the akaganéite structure, looking approximately down **b**. The small circles represent the H atoms, and the larger circles in the tunnel region indicate Cl anions.

mg sample, and the small sample size sufficiently reduced the H incoherent scattering, and thereby increased the peak to background intensity ratio, to allow successful refinement of the data.

It is well known from previous studies that akaganéite transforms into hematite when heated to ~300 °C (e.g., Mackay 1960; Morales et al. 1984). The details of the mechanism of this structural transformation, however, are not well understood. Some studies have suggested the possibility of an intermediate maghemite phase (Meroño et al. 1985). Also, some differential scanning calorimetry (DSC) experiments have shown a significant exotherm at ~525 °C that has not been satisfactorily explained (Morales et al. 1984). In the second part of our study, we used temperature-resolved real-time synchrotron X-ray powder diffraction and Rietveld refinements, along with temperature-resolved Fourier transform infrared spectroscopy (FTIR), to investigate changes in the akaganéite structure and its transformation into hematite as it was heated from 26 to 800 °C.

DATA COLLECTION AND REFINEMENT

Data collection

The sample used in this study was the same as that used by Post and Buchwald (1991), and includes a minor impurity of goethite (~6 wt%). It formed as a corrosion crust on the Campo del Cielo iron-nickel meteorite, and analyses by Post and Buchwald (1991) yielded the chemical formula $Fe^{3+}_{7.6}Ni^{2+}_{0.4}O_{6.35}(OH)_{9.65}Cl_{1.25}{\cdot}nH_2O$. The sample was hand ground under acetone in an agate mortar and passed through a 400 mesh sieve. A ~100 mg sample was loaded into a 2 mm quartz capillary for neutron diffraction data collection. A second akaganéite sample, also from the Campo del Cielo meteorite, but with no goethite impurity, was loaded into 0.5 mm quartz capillaries for the synchrotron X-ray diffraction study. The room temperature time-of-flight neutron diffraction experiment was performed at the Manuel Lujan Jr. Neutron Scattering Center at the Los Alamos National Laboratory. Data were collected for 21.6 h with the high intensity powder diffractometer (HIPD) with four detector banks centered at ±90° 2θ and ± 153.4° 2θ. The X-ray diffraction data were collected at beam line X7B of the National Synchrotron Light Source (NSLS), Brookhaven National Laboratory (BNL), using a wavelength of 0.9273 Å. Different samples were heated in air and under vacuum using a Blake Instruments furnace with a Pt-13%Rh coiled wire yoke encased in ZrO_2 cement (Brown et al. 1973). The temperature was varied with an Omega controller and monitored with a Chromel-Alumel thermocouple located ~2 mm from the specimen. The actual sample temperature was determined for the range 26 °C to 1000 °C by a variety of phase and melting transitions and by the placement of an additional thermocouple in the sample position. The highly linear relationship between the observed and actual temperatures ($r^2 = 0.983$) allowed us to calculate a calibration curve with an estimated error of ±5 °C for a given temperature. Temperature resolved data from 26 °C to 800 °C were collected as a series of 120 s exposures with a MAR345 full imaging plate detector. The temperature was increased continuously at 5.2 °C/min and measurements were obtained every ~17 °C, due to down time for reinitializing the sample rotation angle and reading the imaging plate. Thus, each exposure encompassed a temperature range of ~10.4 °C. During each exposure the sample was rotated through a 120° angle. Any preferred orientation of the powder should have been eliminated through a combination of specimen rotation, use of a capillary sample holder, and full intensity integration of the diffraction rings, as obtained using the program Fit2D (Hammersley et al. 1996) with a polarization factor of 0.93.

The transmission infrared spectroscopy data were collected using a Bio-Rad FTS3000 spectrometer with attached UMA-500 microscope that uses an MCT detector. The high-temperature study was carried-out using a Linkham Scientific Instruments FTIR600 heating stage with a TMS94 controller. Approximately 2 mg of the akaganéite powder dispersed in water was evaporated onto a BaF_2 disc, which was loaded into the heating stage. The heating stage sample chamber was sealed top and bottom with BaF_2 windows and purged throughout the heating experiment with dried and CO_2-scrubbed air. The sample was heated from 26 to 100 °C at 10 °C per minute, and from 100 to 320 °C at 5 °C per minute. Spectra were collected every 50 °C from 100 to 250 °C, and every 10 °C above 250 °C. Background spectra were collected at temperature from a sample-free area of the BaF_2 disc. The temperature was monitored by a platinum resistor sensor to a stated accuracy of ±0.1 °C, and measurements made for a variety of known melting and solid-state phase transitions showed the thermocouple temperature was accurate to within approximately ±2 °C.

Structure refinement

The Rietveld refinements were performed using the General Structure Analysis System (GSAS) of Larson and Von Dreele (2001). The starting structural parameters were taken from Post and Buchwald (1991). For the neutron refinement, the data from the +90° detector bank were used. The backgrounds for the X-ray and neutron diffraction patterns were fit

using a linear interpolation function and cosine series function, respectively. Peak profiles in the neutron data were approximated using the profile convolution function of Von Dreele et al. (1982), and the X-ray peaks were modeled by a pseudo-Voigt profile function as parameterized by Thompson et al. (1987) with asymmetry corrections by Finger et al. (1994) and microstrain anisotropic broadening terms by Stephens (1999). Temperature factors for a given atom type were constrained to be equal. For the goethite impurity in the neutron pattern, the peak profile parameters were set equal to those of akaganéite and only the scale factor was refined.

During the initial cycles of refinement using the neutron data, only the background, scale, peak profile, and unit-cell parameters were allowed to vary. After convergence, a difference Fourier map was calculated in order to locate the H atom positions. The H atoms were added to the structure model and all atom positions and temperature factors and Cl and H occupancy factors were refined. The large displacement factor refined for the Cl atom suggested the possibility that the site might be split along the tunnel direction. Subsequent refinement using a split site model, with the Cl displaced by ~0.4 Å, resulted in a significantly lower displacement factor (U_{iso} = 0.075 vs. 0.12) and improved R_{wp}. Soft constraints were used to limit the Fe-O bond distances to within the range observed for goethite (1.95–2.09 Å) by Szytuta et al. (1968). The weighting factor for the constraints was gradually reduced and set to zero during the final stages of the refinement. The final refinement parameters are listed in Table 1, atom positions in Table 2, and corresponding bond distances in Table 3. The final observed, calculated, and difference neutron powder diffraction patterns are plotted in Figure 2. As is often the case, the standard deviations calculated by GSAS for the lattice parameters are lower than the true errors (Post and Bish 1989). We present the errors calculated by GSAS in the tables and figures of this paper with the understanding that the systematic errors may be more than an order of magnitude higher than the calculated deviations.

Rietveld refinements using the synchrotron powder X-ray diffraction data collected in air were completed for room temperature and for a range of temperatures up to the point at which akaganéite decomposed and hematite started to form (~310 °C). The room-temperature refinements using neutron and X-ray data yielded nearly identical structures, but because the neutron refinement yielded atom positions with greater precision and included H atom positions as well, only the neutron diffraction values are reported in Table 2. The final parameters for the room temperature X-ray refinement are included in Table 1, and the corresponding observed, calculated, and difference diffraction patterns are plotted in Figure 3.

Discussion

The Rietveld refinements for akaganéite using room-temperature neutron and synchrotron powder diffraction data, respectively, confirm a monoclinic structure, at least for this sample, as reported by Post and Buchwald (1991). Overall, our results compare well with those reported by Post and Buchwald (1991), but the increased precision offered by our neutron study permits a more detailed analysis of the structure.

Table 1. Final Rietveld refinement parameters for akaganéite at 26 °C

	Neutron	X-ray
Space group	*I*2/*m*	*I*2/*m*
	Unit cell	
a (Å)	10.587(1)	10.5876(5)
b (Å)	3.0311(2)	3.03357(8)
c (Å)	10.515(1)	10.5277(6)
β (°)	90.03(4)	90.14(2)
V (Å^3)	337.44(6)	338.13(2)
	Refinement	
No. of data points	2876	2173
No. of reflections	452	251
Diffraction range (σ Å)	0.8–12	1.0–12
No. of variables	43	65
R(F^2)	0.049	0.015
R_{wp}	0.019	0.016
χ^2	1.97	2.56

Table 2. Atomic coordinates and isotropic displacement factors for akaganéite (neutron)

Atom	*x*	*y*	*z*	Site occupancy factor	U_{iso} (Å^2) × 100*
Fe1	0.8544(6)	0	0.3424(6)	1.0	0.0167(3)
Fe2	0.3452(7)	0	0.1450(5)	1.0	0.0167(3)
O1	0.663(1)	0	0.2883(7)	1.0	0.0122(4)
O2	0.662(1)	0	0.0429(8)	1.0	0.0122(4)
O3	0.2946(8)	0	0.3351(9)	1.0	0.0122(4)
O4	0.0374(7)	0	0.325(1)	1.0	0.0122(4)
Cl	0	0.132(4)	0	0.42(1) †	0.075(2)
H1	0.367(2)	0.098(4)	0.626(1)	0.5	0.009(2)
H2	0.348(2)	0.056(6)	0.405(1)	0.5	0.009(2)
H3	–0.105(3)	0	0.122(4)	0.32(3)	0.009(2)

*Isotropic displacement factors for same atom types were constrained to be equal.
† Occupancy factor for Cl was 0.29(1) from Rietveld refinement using X-ray data.

Table 3. Selected bond distances (Å) for akaganéite (neutron)

Fe1-O1	2.11(1)	Fe2-O3	2.07(1)
Fe1-O1	2.054(7) × 2	Fe2-O3	2.13(1) × 2
Fe1-O2	1.944(7) × 2	Fe2-O2	1.98(1)
Fe1-O4	1.95(1)	Fe2-O4	1.985(7) × 2
<Fe1-O>	2.01	<Fe2-O>	2.05
H1-O1	1.02(2)	H2-O3	0.94(2)
H1-O1	2.90(1)	H2-O2	2.78(2)
H1-O2	2.65(2)	H2-O2	2.95(2)
H1-O2	2.97(2)	H2-O3	3.00(2)
H1-Cl	2.08(2)	H2-Cl	2.11(2)
H1-Cl	2.38(2)	H2-Cl	2.29(2)

Octahedral sites

Both symmetrically distinct Fe-O octahedra in akaganéite are distorted, with Fe-(O, OH) distances ranging from 1.94 to 2.11 Å for Fe1 and from 1.98 to 2.13 Å for Fe2 (Table 3). The mean Fe-(O, OH) distances are 2.01 and 2.05 Å for Fe1 and Fe2, respectively. These values are similar to Fe-(O,OH) distances in goethite (α-FeOOH), which range from 1.95 to 2.09 Å, with a mean value of 2.02 Å (Szytuta et al. 1968). In goethite, the three longer Fe-O bonds are to the OH^- groups and the three shorter bonds to O atoms. The reduced effective charge for O in OH^- results in longer Fe-O distances. Both Fe octahedra in akaganéite also show three longer and three shorter Fe-O distances (Table 3), and the longer distances are to the O1 and O3 sites, which, as is discussed below, are the OH^- anions. The Fe cations are displaced from their polyhedral centers, probably due to cation-cation repulsions between adjacent octahe-

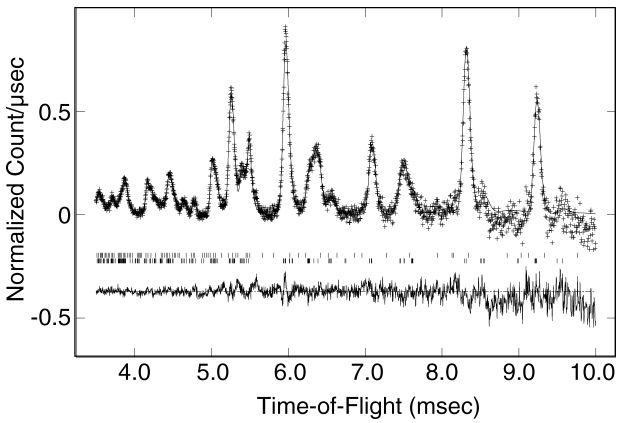

FIGURE 2. Final observed (crosses), calculated (solid line), and difference (lower) powder diffraction patterns for the Rietveld refinement using the neutron powder diffraction data. The background has been subtracted and the intensities have been normalized to the incident spectrum.

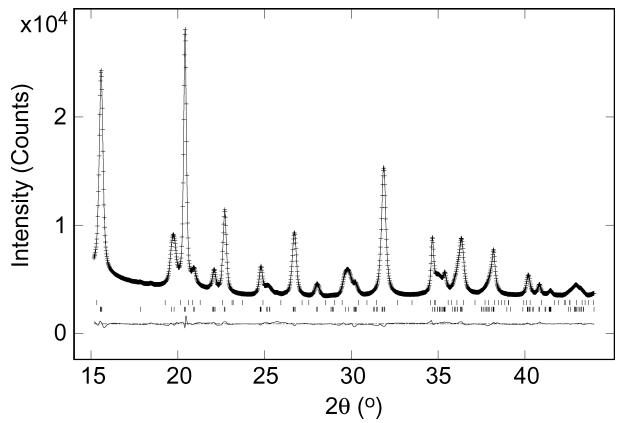

FIGURE 3. Final observed (crosses), calculated (solid line), and difference (lower) powder diffraction patterns for the Rietveld refinement using the 26 °C synchrotron powder X-ray data.

dra. Similar displacements were observed in akaganéite by Post and Buchwald (1991) and have been reported for other phases having the hollandite structure (e.g., Post et al. 1982).

The chemical formula determined by Post and Buchwald (1991) indicates that for this akaganéite sample an average of ~5% of the Fe^{3+} is replaced by Ni^{2+}. Because Fe and Ni have similar X-ray scattering factors and neutron scattering lengths, during the refinements we assumed only Fe at the octahedral sites. In order to maintain charge balance, for every Ni^{2+} an additional H^+ cation must added to the structure, as an OH^- group or H^+ atom (e.g., in the tunnels as HCl), or a Cl^- anion must be removed. Chemical analyses performed by Post and Buchwald (1991) did not show a correlation between Cl and Ni contents, and they concluded that the Ni charges were offset by additional H^+ atoms.

H atoms

Difference Fourier maps calculated using the powder neutron diffraction data clearly show H atom positions, H1 and H2, near O1 and O3, respectively (Fig. 4). The O1 and O3 atoms are at the midpoints of the tunnel edges (Fig. 1), and as such are comparable to the positions of hydroxyl O atoms in goethite (Szytuta et al. 1968) and groutite (Glasser and Ingram 1968). The refined H atom positions match well those derived by Post and Buchwald (1991) using structure energy calculations. The refinement indicated that the H positions are split above and below the mirror plane at y = 0, and that each set of split sites is fully occupied. The O-H distances of 1.01 and 0.94 Å (Table 3) compare well with typical O-H distances observed in other structures. The O-H vectors point almost directly toward the Cl sites at the center of the tunnel. Weak hydrogen bonds likely form between O1 or O3 and Cl.

Infrared spectroscopic studies of synthetic akaganéite by Weckler and Lutz (1998) revealed two OH stretch bands that they interpreted as arising from two hydrogen bonds of different strengths to the Cl anions (O-H···Cl). A stronger bifurcated hydrogen bond results if both tunnel sites on either side of a particular H atom (Fig. 5) are occupied, and a weaker bond if one of the adjacent Cl anion sites is vacant. The interionic H···Cl distances derived by Weckler and Lutz (1998) from the IR data are 2.41 and 2.23 Å, respectively, which compare reasonably well with the values determined from our neutron refinement, which range from 2.08 to 2.38 Å. Based on the relative intensities of the two OH bands, Weckler and Lutz (1998) concluded that there are twice as many linear as bifurcated OH···Cl bonds, exactly as is predicted assuming an ordering scheme with every third Cl site vacant in a particular tunnel. Their IR study

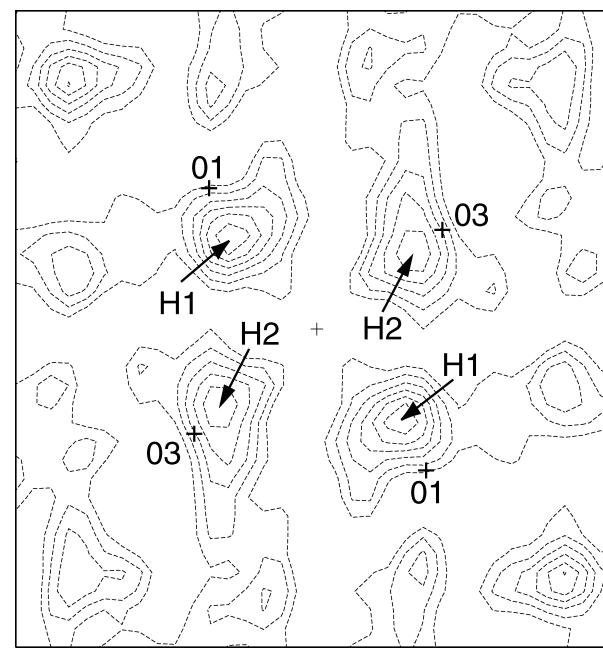

FIGURE 4. Difference Fourier map calculated for neutron powder diffraction data using only the akaganéite octahedral framework as the model structure, at $y = 0$. For clarity, only the negative contours are plotted. The contour interval is 0.1 scattering units.

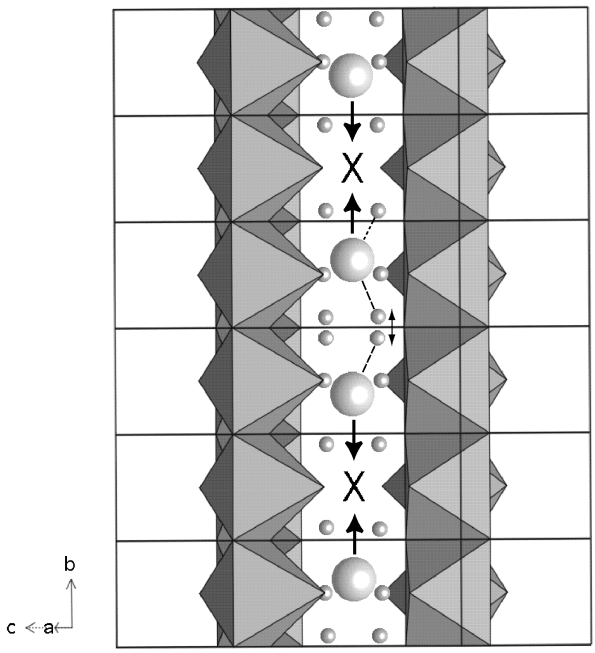

FIGURE 5. Schematic drawing showing a possible Cl anion ordering scheme in the akaganéite tunnels. The small circles represent the H atoms, and the larger circles in the tunnel region indicate Cl anions. Vacant tunnel sites are indicated by "X".

also indicated that the hydrogen bonds in akaganéite are weaker than those in goethite (α-FeOOH) or lepidocrocite (γ-FeOOH) since Cl^- anions are much weaker hydrogen bond acceptors than OH^- or O^{2-} anions. The weaker hydrogen-bonding scheme is undoubtedly a major reason why akaganéite is less thermally stable than the other FeOOH polymorphs. Weckler and Lutz (1998), for example, determined that the heat of decomposition of akaganéite is half as large as and its decomposition temperature is considerably lower than that for the other polymorphs.

In order to achieve charge balance, the chemical formula for our specimen requires 9.4 H atoms per unit cell. The fully occupied H1 and H2 sites account for only 8 of these, leaving 1.4 H atoms elsewhere in the structure. The neutron difference Fourier map shows a weak, but well-defined negative intensity peak that might correspond to an additional H position (H3) in the tunnels. The refined occupancy factor for H3 is ~0.32, equivalent to ~1.28 H atoms per unit cell. If H3 is in fact a H atom position, and not an artifact, it accounts for nearly all of the remaining H atoms. The H3 site is 1.90 Å from the nearest O atom (O1) and 1.75 Å from the Cl anion.

Tunnel site

The Cl anion is located in the tunnel near the center of a prism defined by the eight H atoms that form the hydroxyl groups with O1 and O3 atoms (Fig. 1). Post and Buchwald (1991) placed the Cl anion at (0, 0, 0), but in the current study, we refined a split site with the Cl anion displaced by ~0.4 Å along *b*. The chemical analyses by Post and Buchwald (1991) determined an average of ~1.25 Cl anions per unit cell, filling ~2/3 of the tunnel sites. This Cl occupancy suggests an ordering scheme in a given tunnel with every third tunnel site vacant, which is consistent with conclusions based on the IR results discussed above. Such an arrangement allows the Cl anions to increase their separation distance along a tunnel by moving away from one another toward their respective adjacent vacancies (Fig. 5). This movement increases the Cl-Cl separation from 3.03 Å to a more typical value of ~3.83 Å, thereby reducing the Cl-Cl repulsion. The observed split H1 and H2 sites likely are a consequence of the Cl anion displacements. The H positions in a given cell correlate with the position of the local Cl anion.

The neutron refinement yielded an occupancy of ~1.6 Cl anions per unit cell, suggesting that either this sample has more Cl than the average for this specimen as reported by Post and Buchwald (1991), or that H_2O molecules fill some of the tunnel sites not occupied by Cl anions. Previous studies have proposed that H_2O molecules might occur in akaganéite tunnels, although our IR spectroscopy studies and those by Keller (1970) show evidence of only minor amounts of H_2O. Another explanation is that the $^{35}Cl/^{37}Cl$ isotope ratio in this akaganéite sample is greater than the mean seawater ratio, which is the assumed value for the average neutron scattering length used in our refinement. An increased amount of ^{35}Cl, which has a significantly greater neutron scattering length than does ^{37}Cl, could, perhaps, at least partially explain the larger apparent Cl occupancy factor. This latter explanation is consistent with the fact that our room temperature refinement using X-ray diffraction data gave a Cl occupancy close to the analyzed value.

HEATING EXPERIMENTS

Our synchrotron X-ray diffraction data showed that akaganéite, in air and vacuum, started to transform to hematite in the temperature range 290 to 310 °C (Fig. 6). Rietveld refinements using the data collected in air revealed no significant thermal expansion of the akaganéite structure to ~225 °C (Fig. 7). Above this temperature, the unit-cell volume gradually decreased, primarily in response to decreases in *c* and *b* and an increase in the β angle. The *a* parameter remained nearly constant until ~225 °C and increased at higher temperatures.

In addition to the changes in the unit-cell parameters described above, at ~200 °C the overall intensity of the akaganéite diffraction pattern (as represented by the refined scale factor) started to decrease, suggesting that some akaganéite was decomposing. The decline in overall peak intensities (and scale factors) with increasing temperature continued to the transformation temperature (Fig. 6).

The temperature-resolved IR spectra show a decrease in the intensities of the OH bands in the 3000–3600 wave numbers region beginning between 150 and 200 °C until they disappear at ~ 300 °C (Fig. 8). Parida (1988) and Cai et al. (2001) observed a sharp decline in the Cl/Fe values from 200 to 300 °C, and this is approximately the same temperature range over which the intensities of the akaganéite X-ray diffraction patterns decreased and disappeared. These observations suggest that the loss of most of the hydroxyl and Cl anions is coincident with, and in fact might trigger, the breakdown of the

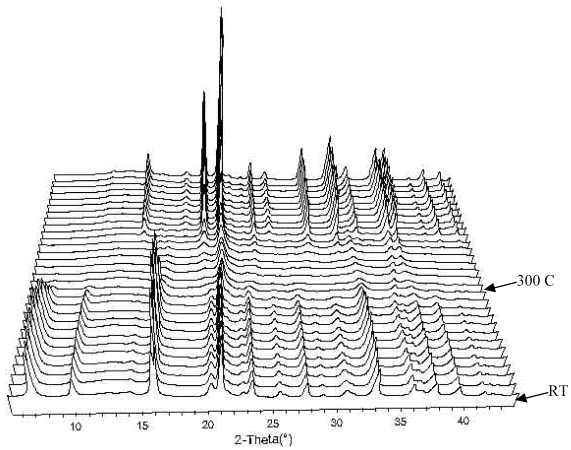

FIGURE 6. Synchrotron X-ray diffraction patterns showing transformation of akaganéite to hematite in air vs. temperature, from 26 to 800 °C.

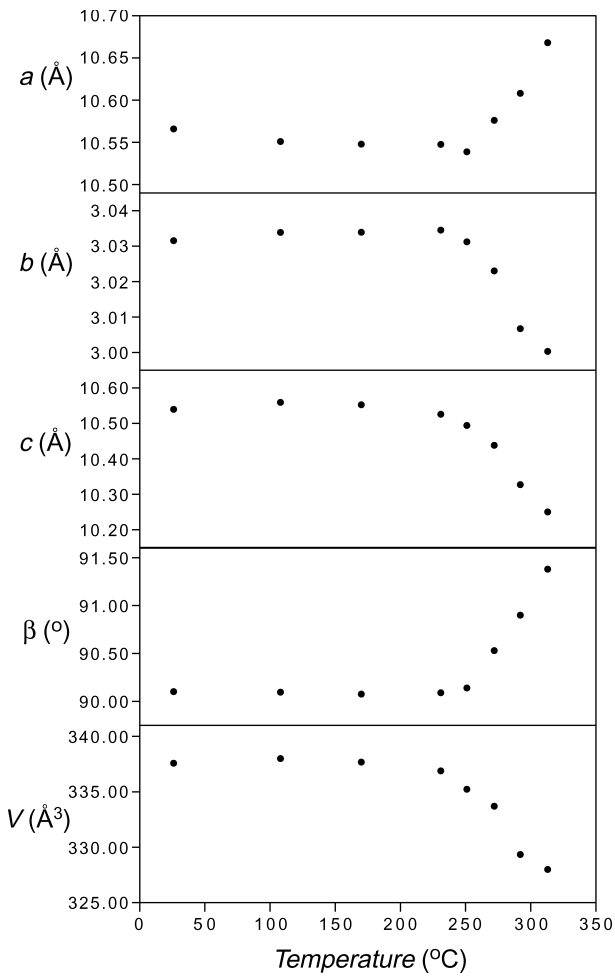

FIGURE 7. Plots of the dependence of the akaganéite unit-cell parameters on temperature.

akaganéite structure. It is interesting, however, that the refined occupancy factors for the tunnel Cl sites in the temperature range 225 to 300 °C are not significantly lower than their room temperature values. Apparently, as akaganéite breaks down at high temperature, Cl is released, but the portion of the sample still contributing to the X-ray diffraction pattern retains its full complement of Cl anions.

The transformation of akaganéite to hematite results in the release of four H_2O molecules per unit cell [$8FeO(OH) \rightarrow 4Fe_2O_3 + 4H_2O$] in addition to Cl. The partial loss of OH molecules from the akaganéite structure during heating likely causes the observed decrease in the *c* and *b* parameters (Fig. 7). As some of the H atoms escape, the associated Fe-O distances contract slightly, due to the shorter Fe-O vs. Fe-OH bond length.

The thermal decomposition of akaganéite has been the subject of several previous studies, with a variety of observations, depending upon the experimental conditions. In vacuum, the decomposition product has been variously identified as maghemite (Mackay 1960; Calbet and Franco 1981) and as an amorphous solid with ultrafine microcrystals of undecomposed akaganéite (Naono et al. 1982). Meroño et al. (1985) described the decomposition product, in vacuum, as a mixture of poorly crystalline maghemite and magnetite that converts to hematite between 440 and 510 °C. On the other hand, Dezsi et al. (1967) and Ishikawa and Inouye (1975) reported that in air akaganéite directly transforms into hematite. Others, however, have noted that the akaganéite structure gradually decomposes into a quasiamorphous state before transforming to hematite (Morales et al. 1984; Meroño et al. 1985).

Our heating experiments in air and vacuum yielded nearly identical results and showed a gradual decomposition of akaganéite, with the first appearance of hematite approximately coincident with the last evidence of crystalline akaganéite. There was no evidence of a maghemite intermediate phase for either heating experiment. We did observe in both cases, however, the presence of very weak diffraction peaks in the range

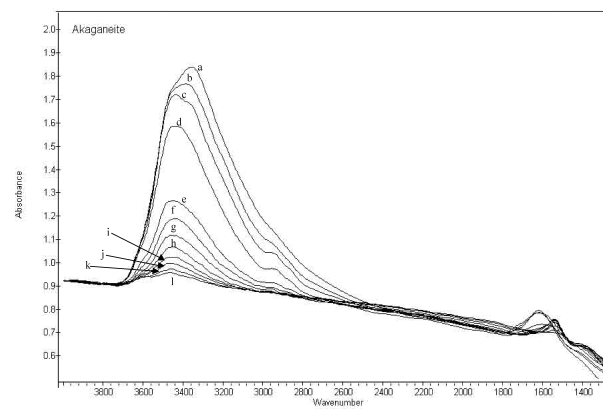

FIGURE 8. Temperature-resolved IR spectra show a decrease in the intensities of the OH bands in the region of 3000-3600 wave numbers starting at ~200 °C. (**a**) 26 °C, (**b**) 100 °C, (**c**) 150 °C, (**d**) 200°C, (**e**) 250 °C, (**f**) 260 °C, (**g**) 270 °C, (**h**) 280 °C, (**i**) 290 °C, (**j**) 300 °C, (**k**) 310 °C, and (**l**) 320 °C.

of ~290 to 325 °C, corresponding to *d*-spacings of 4.1, 3.1, and 3.0 Å, respectively (corresponding to 2θ values of 13.2°, 17.4°, and 18.0°, respectively in Fig. 6). These peaks do not arise from akaganéite or hematite, and we were not able to match them to any known Fe oxides. Morales et al. (1984) observed a change in crystallite size and shape and decrease of microstrain as the newly formed hematite was heated from 300 to 525 °C, and ascribed an exothermic peak in DTA and DSC plots at ~510 °C to recrystallization of hematite. Although we also saw a steady increase in the intensities and a sharpening of the hematite diffraction peaks with increasing temperature above ~310 °C, we did not see any notable changes that might explain the exothermic peak.

In the range of approximately 290 to 310 °C, the akaganéite diffraction pattern essentially disappeared and hematite diffraction peaks appeared (Fig. 6). The hematite peaks sharpened and increased in intensity as the samples were heated to 800 °C, the maximum temperature for our heating experiment. The relatively narrow temperature range encompassing the transformation from akaganéite to hematite and the coincidence of several of the akaganéite and hematite diffraction lines seem to argue for a mechanism that builds the hematite structure from that of akaganéite, as opposed to a model in which hematite rises from an amorphous remnant of the destroyed akaganéite framework. Gualtieri and Venturelli (1999) similarly noted that in the transformation of goethite to hematite close structural relationships between the phases are preserved.

ACKNOWLEDGMENTS

Support for this research was provided by NSF grant NSF EAR01-25908. Brookhaven National Laboratory and the National Synchrotron Light Source are supported under contract DE-AC02-98CH10886 with the U.S. Department of Energy by its Division of Chemical Sciences, Office of Basic Energy Research. Crystal structure drawings were produced using CrystalMaker 5.0 by D. Palmer. We gratefully acknowledge R. Isaac for his valuable assistance with the IR heating experiments, and C. Cahill, R. Downs, J. Rakovan, and P. Burns for their careful and constructive reviews.

REFERENCES CITED

Brown, G.E., Sueno, S., and Prewitt, C.T. (1973) A new single-crystal heater for the precession camera and four-circle diffractometer. American Mineralogist, 58, 698–704.

Buchwald, V.F. and Clarke, R.S., Jr. (1989) Corrosion of Fe-Ni alloys by Cl-containing akaganéite (β-FeOOH): the Antarctic meteorite case. American Mineralogist, 74, 656–667.

Cai, J., Liu, J., Gao, Z., Navrotsky, A., and Suib, S.L. (2001) Synthesis and anion exchange of tunnel structure akaganéite. Chemistry of Materials, 13, 4595–4602.

Calbet, J.M.G. and Franco, M.A.A. (1981) Structural porosity of synthetic akaganéite. Journal of Inorganic Nuclear Chemistry, 43, 257–263.

Dezsi, I., Keszthelyi, L., Kulgawczuk, D., Molnar, B., and Eissa, N.A. (1967) Mossbauer study of beta- and delta-FeOOH and their disintegration products. Physica Status Solidi, 22, 617–622.

Finger, L.W., Cox, D.E., and Jephcoat, A.P. (1994) A correction for powder diffraction peak asymmetry due to axial divergence. Journal of Applied Crystallography, 27, 892–900.

Glasser, L.S.D. and Ingram, L. (1968) Refinement of the crystal structure of groutite, α-MnOOH. Acta Crystallographica, B24, 1233–1236.

Gualtieri, A.F. and Venturelli, P. (1999) In situ study of the goethite-hematite phase transformation by real time synchrotron powder diffraction. American Mineralogist, 84, 895–904.

Hammersley A.P., Svensson S.O., Hanfland M., Fitch A.N., and Hausermann D. (1996) Two-dimensional detector software: From real detector to idealised image or two-theta scan. High Pressure Research, 14, 235–248.

Holm, N.G., Dowler, M.J., Wadsten, T., and Arrhenius, G. (1983) β-FeOOH-Cl (akaganéite) and $Fe_{1-x}O$ (wüstite) in hot brine from the AtlantisII deep (Red Sea) and the uptake of amino acids by synthetc β-FeOOH-Cl. Geochimica et Cosmochimica Acta, 47, 1465–1470.

Ishikawa, T. and Inouye, R. (1975) Role of chlorine in beta-FeOOH on its thermal change and reactivity to sulfur-dioxide. Bulletin of the Chemical Society of Japan, 48, 1580–1584.

Keller, P. (1970) Eigenschaften von $(Cl,F,OH)_{<2}Fe_8(O,OH)_{16}$ und Akaganéite. Neues Jahrbuch für Mineralogie Abhandlungen, 113, 29–49.

Larson, A.C. and Von Dreele, R.B. (2001) GSAS-General Structure Analysis System. Los Alamos National Laboratory Report No. LAUR 86–748.

Mackay, A.L. (1960) β-ferric oxyhydroxise. Mineralogical Magazine, 32, 545–557.

Meroño, M.D., Morales, J., and Tirado, J.L. (1985) Thermal behavior of synthetic akaganéite under different experimental conditions. Thermochimica Acta, 92, 525–528.

Morales, J., Tirado, J.L., and Macias, M. (1984) Changes in crystallite size and microstrains of hematite derived from the thermal decomposition of synthetic akaganéite. Journal of Solid State Chemistry, 53, 303–312.

Naono, H., Fujiwara, R., Sugioka, H., Sumiya, K., and Yanazawa, H (1982) Micropore formation due to thermal decomposition of acicular micro-crystals of beta-FeOOH. Journal of Colloid Interface Science, 87, 317–332.

Parida, K.M. (1988) Physico-chemical characteristics of thermally treated akaganéite (β-FeOOH). Journal of Material Science, 23, 1201–1205.

Post, J.E. and Bish, D.L. (1989) Rietveld refinement of crystal structures using powder X-ray diffraction data. In D.L. Bish and J.E. Post, Eds., Modern Powder Diffraction, 20, 277–308. Reviews in Mineralogy, Mineralogical Society of America, Washington, D.C.

Post, J.E. and Buchwald, V.F. (1991) Crystal structure refinement of akaganéite. American Mineralogist, 76, 272–277.

Post, J.E., Von Dreele, R.B., and Buseck, P.R. (1982) Symmetry and cation displacements in hollandites: structure refinements of hollandite, cryptomelane, and priderite. Acta Crystallographica, B38, 1056–1065.

Stephens, P.W. (1999) Phenomenological model of anisotropic peak broadening in powder diffraction. Journal of Applied Crystallography, 32, 281–289.

Szytuta, A., Burewicz, A, Dimitrijevic, Z., Krasnicki, S., Rzany, H.,Todorovic, J., and Wolski, W. (1968) Neutron diffraction studies of α-FeOOH. Physica Status Solidi, 26, 429–434.

Thompson, P., Cox, D.E., and Hastings, J.B. (1987) Rietveld refinement of Debye-Scherrer synchrotron X-ray data from Al_2O_3. Journal of Applied Crystallography, 20, 79–83.

Von Dreele, R.B., Jorgensen, J.D., and Windsor, C. G. (1982) Rietveld refinement with spallation neutron powder diffraction data. Journal of Applied Crystallography, 15, 581–589.

Weckler, B. and Lutz, H.D. (1998) Lattice vibration spectra. Part XCV. Infrared spectroscopic studies on the iron oxide hydroxides goethite (α), akaganéite (β), lepidochrosite (γ), and feroxyhite (δ). European Journal of Solid State Inorganic Chemistry, 35, 531–544.

MANUSCRIPT RECEIVED JULY 19, 2002
MANUSCRIPT ACCEPTED NOVEMBER 14, 2002
MANUSCRIPT HANDLED BY PETER BURNS